JOURNAL OF MATERIALS SCIENCE 37 (2002) 4391 – 4398

Structural and magnetic properties of room temperature milled $Co_{0.2}Zn_{0.8}Fe_2O_4$ spinel oxide

R. N. BHOWMIK, R. RANGANATHAN
Experimental Condensed Matter Physics Division,
Saha Institute of Nuclear Physics, 1/AF, Bidhannagar, Calcutta 700064, India
E-mail: rnb@cmp.saha.ernet.in
E-mail: ranga@cmp.saha.ernet.in

We report the nanoparticle $Co_{0.2}Zn_{0.8}Fe_2O_4$ spinel oxide, synthesized by room temperature mechanical milling. The system is stabilized mainly in spinel oxide phase after 78 hrs milling time and no other phases have been observed from the XRD spectra of the 100 hrs milled sample. We have studied the particle size effects on structural as well as on magnetic properties by annealing the 100 hrs as milled sample at different temperatures for 12 hours. The XRD and TEM data show that the particle size decreases with increasing milling time upto 60 hrs and then show an increasing trend with milling time. The particle size also increases with annealing the 100 hrs as milled sample with better crystalline structure. It is observed that the magnetic properties of the annealed samples can be correlated with the structural change without breaking the crystal symmetry of the cubic spinel phase of $Co_{0.2}Zn_{0.8}Fe_2O_4$ spinel oxide. The change in the crystal structural as revealed by the XRD spectra can be associated with the non-equilibrium to equilibrium cationic distribution between tetrahedral (A) and octahedral (B) sites of the spinel structure.

1. Introduction

The synthesis of nano particle magnetic materials have been intensively investigated in recent years because of their potential applications in high density magnetic recording, as a carriers in magnetic fluids, and as magnetically guided drug carrier etc. [1]. Various preparation techniques such as Sol gel technique, hydrothermal techniques have been used to prepare nano particle materials. Because of the limitations for large scale production and for preparation of the complex systems by the above mentioned techniques [2], mechanical alloying is becoming a standard procedure to obtain nano sized materials and metastable phases. It has also been found that some materials can not be prepared by high temperature ceramic method. In that cases, the mechanical milling method is very useful for room temperature synthesis of those compound materials. Although theoretical and empirical models of micro structural evolution have been proposed but the fundamental mechanisms involved are not yet fully understood [3]. Several interesting magnetic phenomena of nano particles system under much investigation in recent time are magnetic tunneling [3], superparamagnetism and spin canting [4] effects. There are several reports on a variety of disordered materials, prepared under mechanical milled synthesis, e.g., metals like Fe, Co, Ni [5], metallic alloys like $Co_{2-x}Fe_xGe$ [6] and oxides like $Mn_{0.5}Zn_{0.5}Fe_2O_4$ [7] and $ZnFe_2O_4$ [8, 9]. Del Bianco *et al*. [10] have studied the grain boundary structure of ball milled iron particles through magnetization and Mössbauer spectroscopy measurements. They observed the increase of micro strain during milling of the Fe powder and attributed the change in magnetic properties due to interactions between ferromagnetic nano particles and an antiferromagnetic or disorder grain (particle) boundary phases. They also suggested that the lattice deformation and slight deviation from spherical shape of the particles may also increase the shape anisotropy and strain induced anisotropy of the milled materials. The relaxation of the micro strain and release of excess enthalpy upon subsequent annealing of the materials can give rise different non-equilibrium states [10]. However, most of the metal and inter-metallic nano particle systems are not chemically stable in atmospheric conditions, hence their applications are limited [11], in comparison with the relatively atmospheric stable oxides materials.

In this presentation our attention will be focussed mainly on spinel oxides materials. In spinel lattices the anions (O^{2-}, S^{2-} ions) form a cubic close packing, in which the interstices are occupied by tetrahedral (form A sites or sublattice) and octahedral (form B sites or sublattice) coordinated cations. The interesting aspect of the spinel oxide is that the total magnetization ($M = M_B\cos\theta - M_A$, θ is the canting angle between B site moments) depends on the magnetic ions distribution in B and A sites and the properties are strongly depend on the competition between various superexchange type interactions via O^{-2} ions i.e., intersublattice superexchange interactions J_{AB} between two

sites ions and intra-sublattice superexchange interactions J_{AA} and J_{BB} between ions of same site. The necessary conditions for long range ordering in the system is $J_{AB} \gg J_{BB} \gg J_{AA}$ [12]. It has been reported [9] that certain amount of site disorder, i.e., the ionic rearrangements between A and B sites in nano particles system in comparison with the bulk system is sufficient to change the super-exchange interactions of the system and gives rise a variety of magnetic structures [4, 13]. According to the core/shell model by Kodama *et al*. [4], a ferromagnetic core exists inside the clusters due to the reduction of canted spin structure whereas the surface spins still remain in canted structure. In general, the magnetization and the ordering temperature decreases with particle size reduction [10, 11] and subsequent annealing of the system will increase the magnetization as well as ordering temperature. But, Tang *et al*. [14] explained the decrease of Curie temperature (T_C) with increasing particle size of $MnFe_2O_4$ system in terms of the finite size scaling effects. On the otherhand P. Zagg *et al*. [15] and V. A. M. Brabers [16] questioned on the finite size scaling effects of $MnFe_2O_4$ system. They argued that the enhancement in T_C with decrease in particle size is due to the non-equilibrium cations distribution between tetrahedral and octahedral sites. The non-equilibrium cation distributions have been well established in most of the spinel oxides like $ZnFe_2O_4$ by S. A. Oliver *et al*. [13]. In the present communication, we wish to study the particle size effects of mechanical milled $Co_{0.2}Zn_{0.8}Fe_2O_4$ spinel oxide based on XRD, TEM and ac susceptibility measurements.

2. Experimental

2.1. Sample preparation and characterization

Nanoparticle $Co_{0.2}Zn_{0.8}Fe_2O_4$ spinel oxide was synthesized at room temperature using Fritsch Planetary Mono Mill "Pulverisette 6". Stoichiometric mixture of ZnO (99.998% from Johnson Matthey), Fe_2O_3 (99.998% from Johnson Matthey) and Co_3O_4(99.5% from Fluka) oxides were taken in a 80 ml steel vial with 10 mm balls. The mixture was crushed and disintegrated in the grinding bowl, keeping the ball to material weight ratio 12 : 1. The rotational speed of the miller was set 300 rpm. Small quantities of sample were taken out from the bowl after 24, 36, 48, 60, 78 and 100 hours of milling in order to check the phase formation during milling time via X ray diffraction (XRD) spectra using Philips PW1710 diffractometer with Cu K_α radiation. The 100 hours as milled sample was then annealed in separate batches at different temperatures ranging 200°C to 1000°C for 12 hours. All the heat treatment work was performed in atmospheric condition with heating and cooling rate 100°C/hour. We have checked the chemical composition as well as the contamination effects during mechanical milling process via X-ray fluorescence technique. A Kevex x-ray tube with a Tungsten anode was used to excite Sr K x-rays from a $SrCo_3$ pellet, used as a secondary target in our X-ray Fluorescence system. Pellet of the 900°C—12 hours annealed sample (diameter 13 mm and thickness 3 mm prepared under the pressure of 1 ton per cm^2) was then irradiated. The entrance and exit angles of x-rays were 45°. The Fluoresecne spectra were recorded using ORTEC HPGe detector and finally fed into a PC based multichannel analyzer. We have also used TEM technique to determine the particle size of our samples. When the crystallite size is less than 100 nm, the term particle size is used [17]. The ac susceptibility measurements were performed using home made ac susceptometer [18].

3. Results

3.1. Structural properties

X ray diffraction spectra of $Co_{0.2}Zn_{0.8}Fe_2O_4$ nanocomposite with different milling time are shown in Fig. 1. The spectra show that the phases of the starting oxides are gradually decreasing and spinel phase appearing prominent with increasing milling time. It is found that the spinel phase becomes dominant after 78 hours milling of the mixed composites. Except spinel phase, no significant impurity phases is observed for the 100 hours milled sample. The XRD lines are broad due to the decrease of particle size into the nano meter range (<100 nm) and also may be due to the non-uniform micro strain in the lattice planes [17, 19]. We have used the 100 hours milled sample for the heat treatment and experimental works. Fig. 2 represent the XRD spectra for the samples which have been annealed at different temperature in the range 200°C to 1000°C for 12 hours. The system stabilizes in a better crystalline phases as a result of heat treatment. The XRD peak lines are also becoming sharp due to the increase of coherent length between different lattice planes, which results the increase of particle size. It should be noted that the crystalline peaks are shifting to lower scattering angle (2θ) with annealing temperature upto 600°C, except a shift to higher scattering angle for 500°C. For

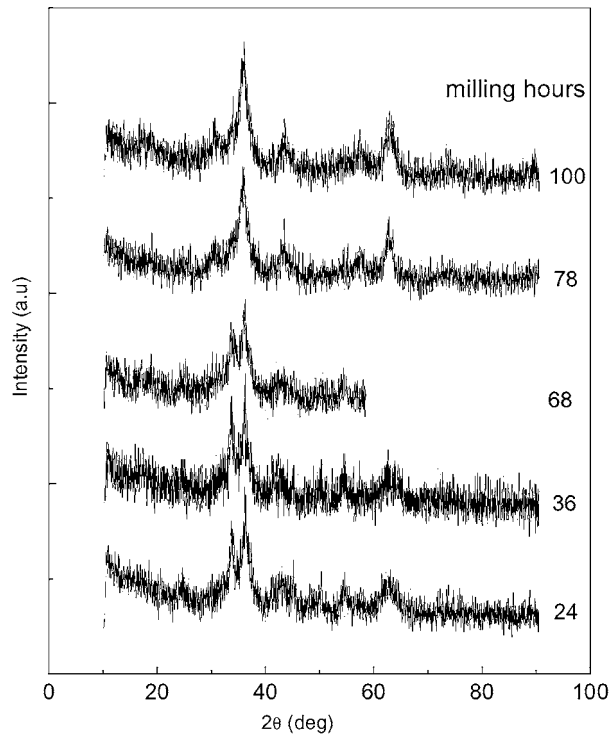

Figure 1 The XRD pattern of mechanically milled $Co_{0.2}Zn_{0.8}Fe_2O_4$ system with different milling time at room temperature.

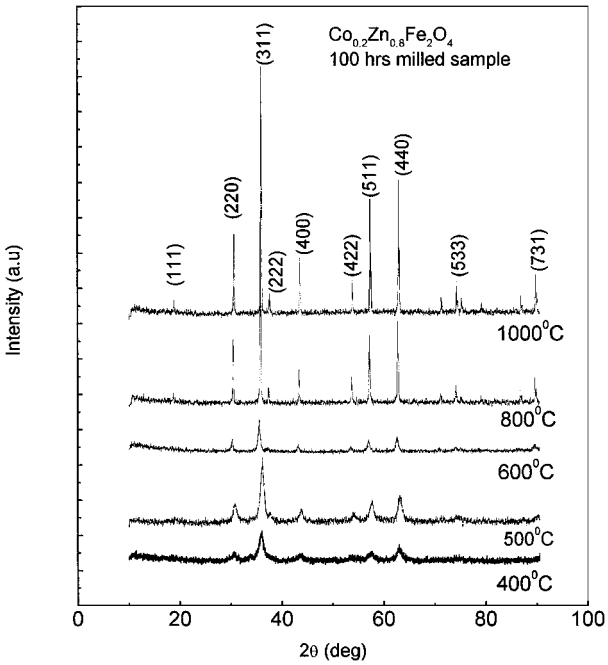

Figure 2 XRD spectra of 100 hrs milled sample which has been annealed at different temperatures.

the samples with annealing temperature above 600°C, the peaks shift to higher scattering angle. The reproducibility of 500°C and 600°C annealed samples have been checked by preparing second batch which shows similar XRD spectra to that of the reported one in Fig. 2. The shift of the XRD peak positions have been illustrated by 311 peaks in Fig. 3. Any kind of distortion, if introduced in the unit cell during milling time, will change the symmetry of the crystal structure and additional peak lines will appear in the XRD spectra. We see in Fig. 2 that there is no extra peak lines, except that for cubic spinel structure. This is possible if the unit cell is expanded or contracted uniformly with maintaining the symmetry of the crystal structure (here cubic spinel structure), the diffraction lines merely shift their positions with out increase in numbers, since no changes in cell symmetry is involved. The most likely change in crystal structure is the rearrangement of Zn^{2+} and Fe^{3+} ions between tetrahedral and octahedral sublattice [13]. This change is highly reflected at the 600°C annealed sample as the spectral intensity is diminished in comparison with the 500°C and 700°C annealed sample. This indicates the system is passing through a disorder-order transformation of the lattice structure in the temperature range 500°C to 600°C [17].

We can draw a schematic diagram (Fig. 4) to correlate the shift of XRD peak and the structural change by assuming the competition between mechanical strain developed during mechanical milling and thermal strain developed due to heat treatment. The planes having small arrows inside the circles represent the lattice planes. Before, heat treatment (Fig. 4a) suppose the lattice planes are compressed in a direction normal to the X-ray reflecting planes due to non-uniform micro strain, which will decrease the inter-planer separation 'd'. When heat treatment works are performed (Fig. 4b), a tensile (thermal) strain will be acted on the lattice planes. If this thermal strain is normal to the

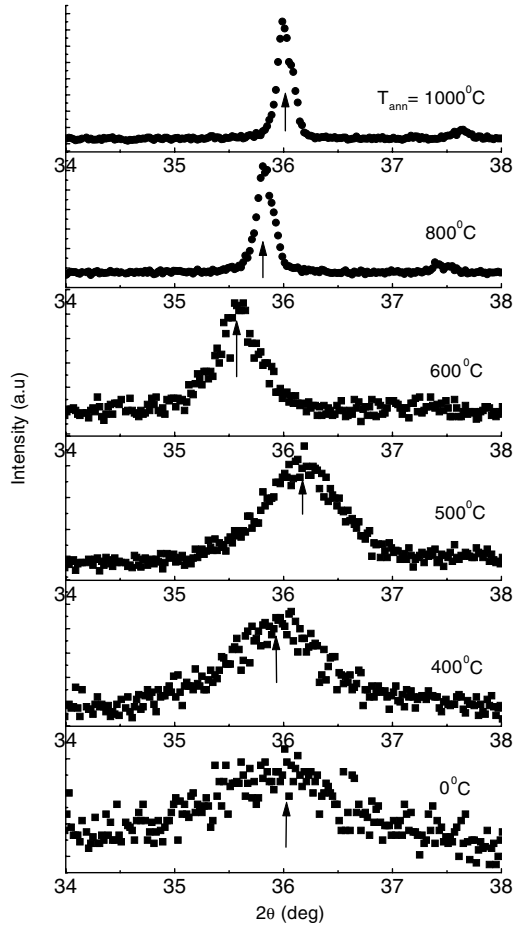

Figure 3 XRD spectra of 311 peak line for 100 hrs milled sample which has been annealed at different temperatures.

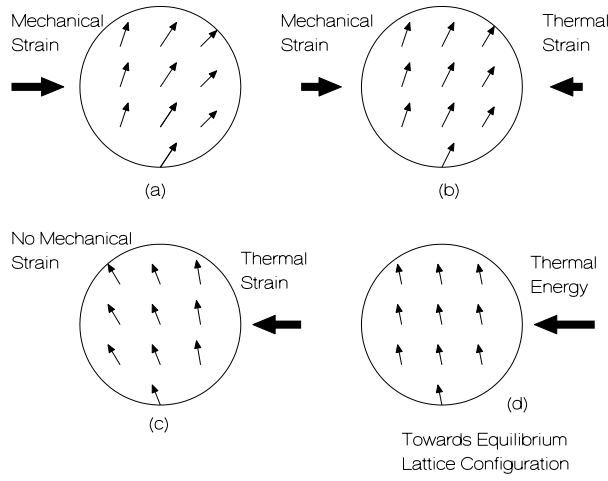

Figure 4 Schematic diagram of competitive process between mechanical strain and thermal strain, (a) to (d) maintain the increased annealing temperature.

lattice plane, the inter-planer separation will increase. As a result the mechanical strain try to be released [10]. It should also be remembered that during this competition between mechanical strain and thermal strain, the elastic property of the lattices will play a significant role [17]. Above a certain annealing temperature (here >400°C), the thermal strain will dominate over the mechanical strain (Fig. 4c). Depending on the elastic vibration of lattice planes, the inter-planer spacing may show oscillating nature and disorder-order

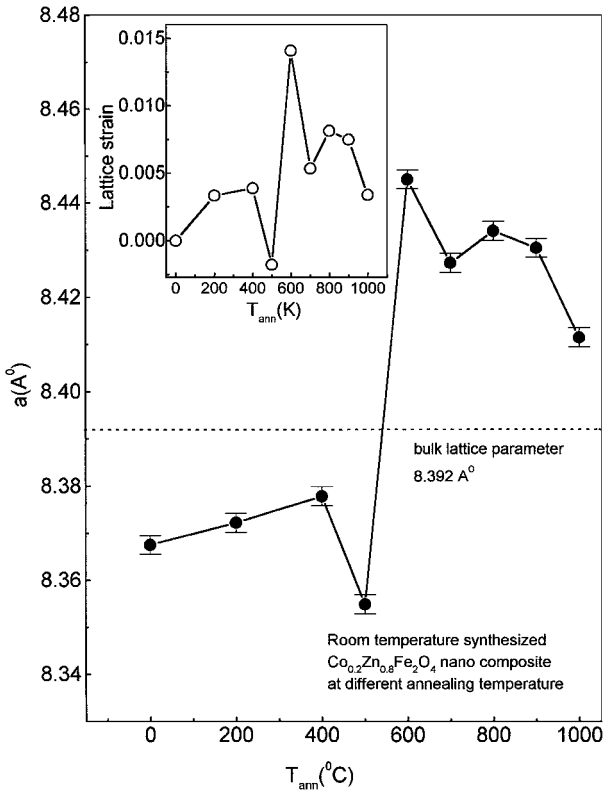

Figure 5 The lattice parameter vs annealing temperature for the heat treated samples. The inset shows the lattice strain with annealing temperature, calculated using 311 peak line shift.

transformation may be observed in the lattice structure (as observed in the temperature range 500°C to 600°C). On further annealing, the system tends toward an equilibrium configuration of the lattices (Fig. 4d). We have calculated the lattice strain as $(d_{h100} - d_{hn})/d_0$, where d_{h100} is the lattice plane spacing for 100 hours as milled sample, $n = 100$ to 1000°C, d_0 is the lattice plane spacing for the bulk sample prepared by solid state method. Fig. 5 inset suggest a non-uniform micro strain in the lattice planes and the lattice strain is released as the sample is annealed above 600°C. The interesting observation (Fig. 5) is that the lattice parameter (Å) is also consistent with the change in peak position with annealing temperatures i.e., lattice parameter is increasing upto 600°C with a small dip at 500°C and then decreasing as the system stabilizes in a better crystalline phase.

The average particle size ($\langle d \rangle$) of the samples have been determined from the (311) peak of XRD spectra using Debye-Scherrer equation: $\langle d \rangle = K\lambda/\beta \cos\theta$, where $K = 0.89$, λ is the X ray wave length = 1.54056 Å for Cu Kα radiation, β is the full width at half-maximum of the spectral line and θ is the angle of diffraction in radian. We have also determined the particle size from the tunneling electron microscope (TEM) photographs (Figs 6 and 7). The amorphous phase or grain boundary phases are not very clearly distinguished from the XRD spectra or

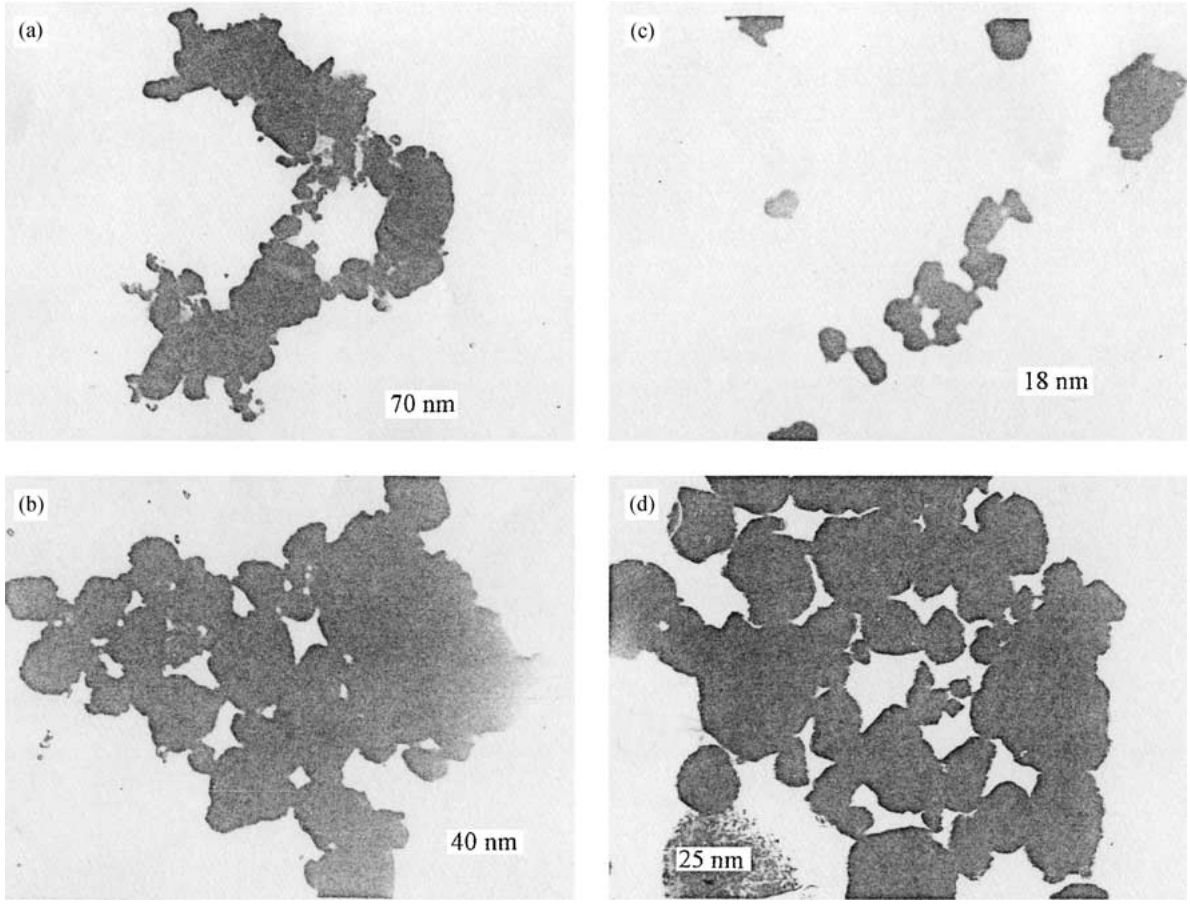

Figure 6 TEM photographs for different milling time (hrs) for $Co_{0.2}Zn_{0.8}Fe_2O_4$ room temperature synthesized spinel. (a) 24 hours, (b) 48 hours, (c) 78 hours and d) 100 hours.

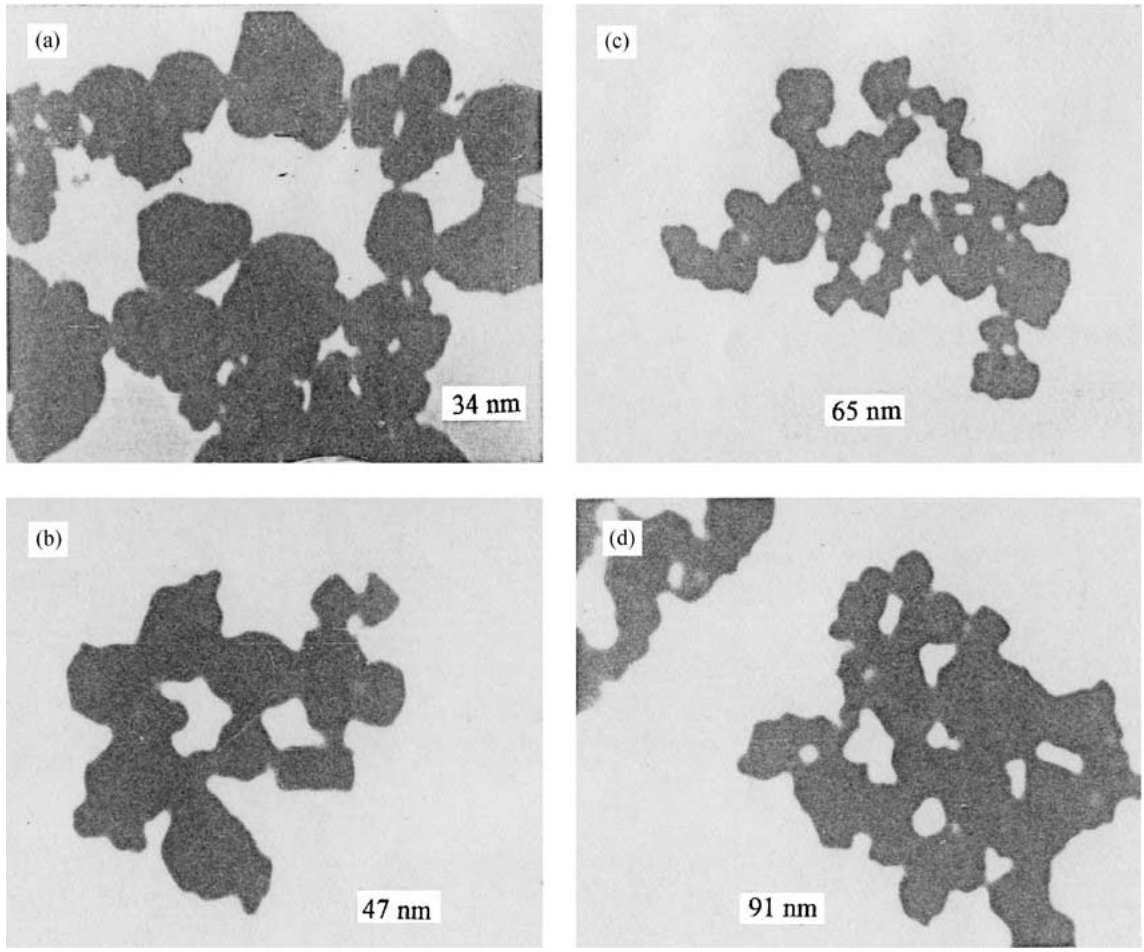

Figure 7 TEM photographs (different magnification factors) for the 100 hours milled and annealed at different temperatures (T_{ann}) for 12 hours. (a) 400°C, (b) 600°C, (c) 800°C and (d) 1000°C.

TEM photographs. The TEM values of $\langle d \rangle$ (consists of grain + grain boundary) are slightly greater than the XRD values of $\langle d \rangle$ (crystallite size). The difference of particle size determined from the XRD and TEM data suggest that a significant fraction of the sample volume is composed of grain (particle) boundaries and interfaces. Fig. 6 shows the transformation from a heterogeneous mixed phase to a more homogeneous phase with well defined particle size. Fig. 7 suggest that the particles are not in ideal spherical shape. Fig. 8a shows that the particle size ($\langle d \rangle$) of the nanocomposite decreases with increasing milling time upto 60 hrs [19] and on further increasing the milling time, the particle size slightly increases due to agglomeration of nano sized particles. We also find in Fig. 8b that the particle size increases by annealing the sample upto 1000°C for 12 hours. Eventhough, a sharp crystalline spectrum is observed at the annealing temperature 1000°C but the particle size is ≈90 nm (TEM data) which is less than the critical particle size (≈100 nm) for nano particle materials [1, 2].

In order to check the chemical composition, we have employed X-ray fluroscence spectroscopy on the 900°C − 12 hours annealed sample. The XRF spectra (Fig. 9) show the characteristic K_α and K_β lines of Fe, Co and Zn. The spectra also show some traces of Cr apart from the above three elements. The peak integrals of the K_α lines of all the elements are obtained using the standard peak fitting program. These peak integrals were then used as the input of another program to get the relative elemental percentage. This program was developed using the principle of Fundamental Parameter Method [20]. The obtained composition is: Fe = 62.01%, Zn = 28.61% and Co = 8.66% which is very close to the therotically expected values i.e., Fe = 63.53%, Zn = 29.76% and Co = 6.71%. A small amount of Cr(0.71%) contamination has been found which may be from the hardened steel ball. The maximum error in determining the chemical composition is ∼10%.

3.2. Magnetic properties

We have measured ac susceptibility data (χ' and χ'') at h_{rms} ≈1 Oe ac field and frequency (ω) = 337 Hz. Fig. 10 shows the ac susceptibility data of samples annealed upto 600°C. These samples show superparamagnetic behaviour. Below the superparamagnetic blocking temperature T_B the magnetic clusters are blocked in different metastable states [21]. The broad maximum in χ' is due to the distribution of the cluster size, some of which may block at $T > T_B$ and some of them block at $T < T_B$, shows an average blocking temperature at T_B. The χ'' maximum at $T < T_B$ reflects a distribution of relaxation time about T_B. Eventhough, the clusters show superparamagnetic type blocking but it is not necessary that they should be non-interacting. The magnetic response must be collective due to the inter-cluster interactions etc., as suggested by D. Fiorani *et al.* [22] for nano size γ-Fe_2O_3 system.

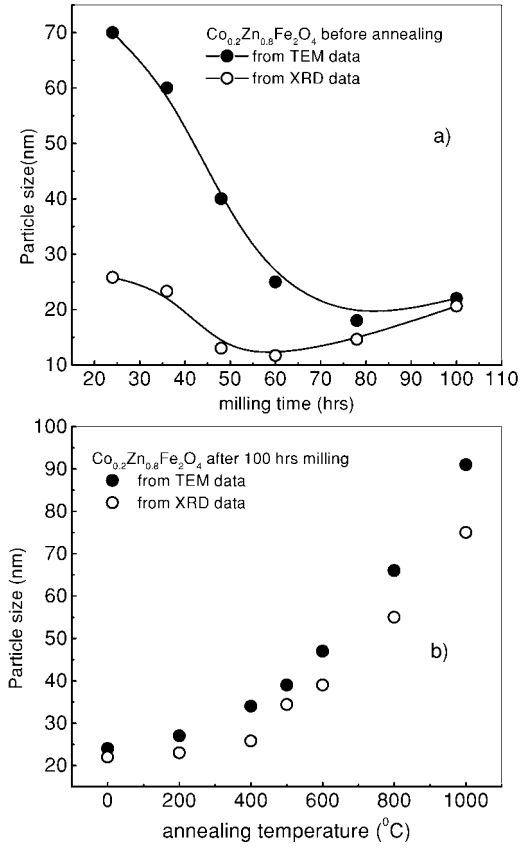

Figure 8 Milling time dependence of particle (grain) size, (b) Annealing temperature dependence of particle (grain) size, obtained from X ray diffraction pattern (311 peak) and TEM data.

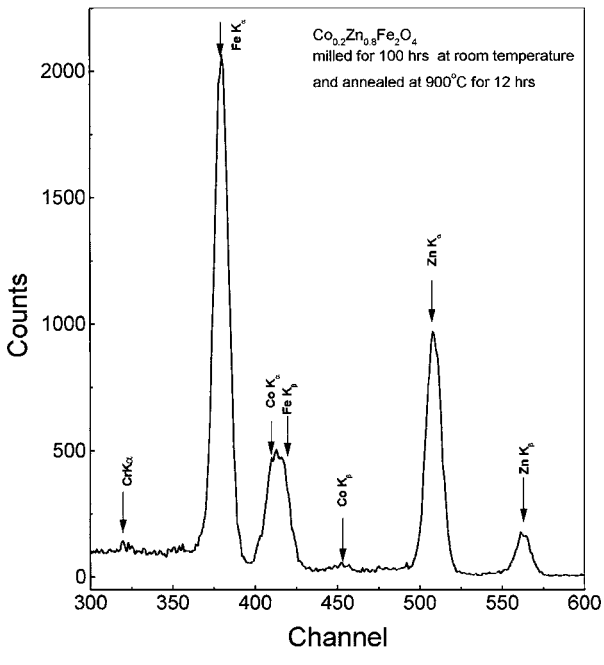

Figure 9 X-ray Fluorescence spectra for the 100 hours milled and 900°C −12 hours annealed sample.

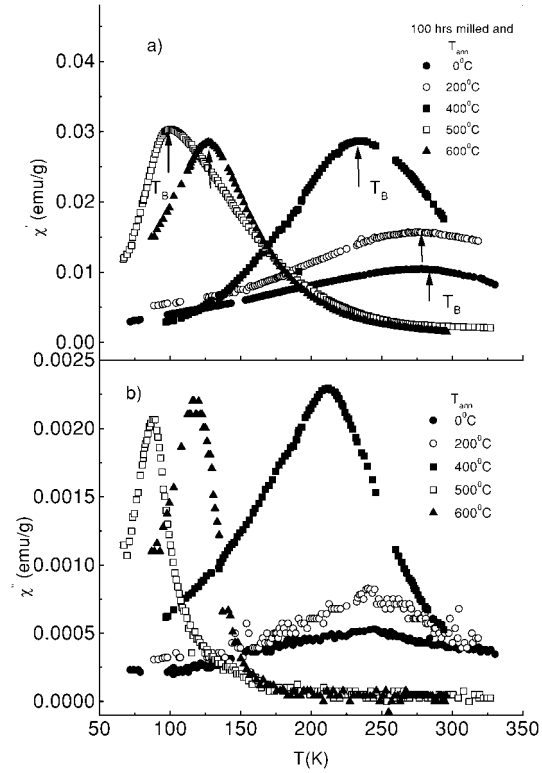

Figure 10 Ac susceptibility data for the 100 hours as milled sample that has been annealed at 200°C to 600°C for 12 hours.

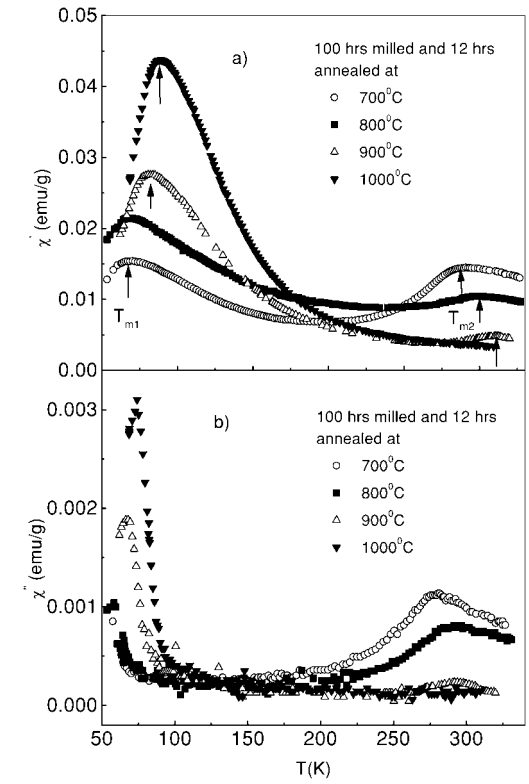

Figure 11 Ac susceptibility data for the 100 hours as milled sample that has been annealed at 700°C to 1000°C for 12 hours.

In Fig. 11 it is observed that the samples annealed at 700°C, 800°C and 900°C shows two maxima. The low temperature maximum occurs at T_{m1} and the high temperature maximum occurs is at T_{m2}. The χ'' data also show two maxima but at slightly lower temperatures with respect to T_{m1} and T_{m2} values. The sample annealed at 1000°C shows a maximum at T_{m1} but no second maximum is observed upto 320 K. We have found from the dc magnetization measurement that the 1000°C annealed shows the signature of second maximum at ≈325 K (details will be published later). This suggest that the high temperature maximum in χ' may be at $T \geq 325$ K for 1000°C annealed sample. However, the bulk sample prepared by solid state

method shows a maximum at the cluster spin freezing temperature $T_{m1} \approx 110$ K and a small shoulder at the short range ferrimagnetic ordering temperature T_{m2} ≈260 K respectively [6]. This means the samples with annealing temperature ≥700°C approaches to the bulk properties and shows two magnetic phases.

4. Discussion

Our results show that the $Co_{0.2}Zn_{0.8}Fe_2O_4$ spinel oxide with particle size ≈20 nm can easily be synthesized at room temperature using mechanical milling. On annealing the 100 hours milled sample, the system stabilizes in a better crystalline structure and the particle size increases to 90 nm for 1000°C −12 hours annealing temperature. The X-ray fluorescence (XRF) spectra does not show any excess amount of Fe due to the contamination effects from hardened steel balls and vial. The small amount of Cr contamination (0.7%) during milling process can not be attributed as a cause of enhancement of magnetic ordering ($T_B \approx 290$ K) for 100 hrs as milled sample in comparison with the short range ferrimagnetic ordering temperature at ≈260 K of bulk sample. The enhancement in ordering temperature with decreasing the particle size has been attributed as a finite size scaling effects [14]. However, from microscopic measurements like Mössbauer spectroscopy it is very much convinced that site exchange between A and B site ions will significantly modify the exchange interactions in spinel oxides [7, 15, 16, 19]. We believe the origin of enhanced magnetic ordering in our 100 hours as milled sample lies in the breakdown of canted spin structure in the B sublattice and ionic redistribution between A and B sites. To clarify this point, we recall that Petitt *et al*. [24] have shown by Mössbauer spectroscopy measurement that in $Co_{1-x}Zn_xFe_2O_4$ the magnetization and ordering temperature decreases for x >0.6 due to the local spin canting in B site. This means if the B site spin canting is reduced, the magnetic ordering will be enhanced [13]. The XRD spectra of the as milled and annealed samples suggest that the most probable internal structural change without changing the symmetry of the cubic spinel structure is the cationic rearrangement that took place during milling and subsequent annealing. In bulk system the ionic distribution is $(Zn^{2+}_{0.8}Fe^{3+}_{0.2})_A[Co^{2+}_{0.2}Fe^{3+}_{1.8}]_BO_4$ [6] and comparable strengths of J_{AB} and J_{BB} allows B site spin canting. Suppose for the 100 hours as milled sample, some Zn^{2+} migrate from A sublattice to B sublattice to replace the same numbers of Fe^{3+} ions from B to A sublattice. Hence, J_{AB} interactions will be enhanced and the B site spin canted structure will be reduced. The significant amount of Zn^{2+} in B sublattice occupancy can be suggested from the low value of lattice parameter of the 100 hour as milled sample in comparison with the bulk sample. On annealing the 100 hours as milled sample, there will be a competition between mechanical strain and thermal strain. As a result a disorder-order structural change is to be expected and is observed in the samples annealed in the temperature range 500°C to 600°C. On further annealing, the recrystallization process forces the system towards an equilibrium lattice configuration.

Besides the cations site exchange, we have to consider the competition between grains and grain boundary effects to explain the magnetic properties. D. L. Pelecky *et al*. [1] proposed that no interactions exist between the smallest size particles. On the other hand, for bulk materials with particle size in the nano scale range the length scale of interactions can span upto many grains and strongly depends on the character of grain boundary phases. The grains will behave like a ferri/ferromagnetic clusters, whereas the grain boundary spins are in a disordered state [4]. When the particle size is small (for annealing temperature ≤600°C in our case), the grains and grain boundary contributions can not be magnetically separated out and a superparamagnetic behaviour is observed. If the annealing temperature is increased the competition between grains (shows ferrimagnetic ordering at high temperature) and grain boundary (shows spin glass freezing/superparamagnetic blocking at low temperature) becomes dominant. This is easily understood from the 600°C annealed sample. The ordering temperature T_B is higher than the 500°C annealed sample but without any two magnetic phases as observed in case of 700°C annealed sample. For the samples annealed at $T \geq 700$°C, the highly disordered grain boundary phases at low temperature is separated out from the high temperature ferro or ferrimagnetic phases of grains. Therefore, the magnetic ordering at high temperature (T_{m2}) is due to the ferri/ferromagnetic ordering of the grains (magnetic clusters) and the clusters will show spin glass freezing or superparamagnetic blocking at T_{m1} due to the intercluster interactions associated with grain boundary effects.

5. Conclusions

We can conclude that the nanoparticle $Co_{0.2}Zn_{0.8}Fe_2O_4$ spinel oxide shows superparamagnetic behaviour when the particle size is small (<40 nm) and the system shows two magnetic phases as the particle size increases by increasing the annealing temperature (≥700°C). Several factors such as surface anisotropy and shape anisotropy influence the magnetic properties upto certain extent. But the non-equilibrium cation distribution in A and B sites and lattice distortion due to mechanical strain are attributed as the main factors for the enhancement of magnetic ordering of 100 hours as milled sample in comparison with the bulk sample. We have proposed a schematic diagram to show how the thermal strain competes with mechanical strain to stabilize a system, prepared under mechanical milling, towards an equilibrium lattice configuration. The structural refinement of the grains and grain boundary phases by annealing the as milled sample approaches to its bulk properties. The detailed study of dc magnetization, ac susceptibility and Mössbauer spectroscopy will be published later.

Acknowledgement

One of the authors RNB thanks Council of Scientific and Industrial Research (CSIR, India) for providing fellowship [F. No. 9/489(30)/98-EMR-I]. We wish to thank Dr. M. Sarkar for providing the X-ray

Fluorescence spectra data and Prof. R. Nagarajan for useful discussion.

References

1. D. LESLIE-PELECKY and R. D. RIEKE, *Chem. Mater.* **8** (1996) 1770.
2. M. GUGLIELMI and G. CARTURAN, *Journal of Non-Crystalline Solids* **100** (1988) 16.
3. J. TEJADA, R. F. ZIOLO and X. X. ZHANG, *Chem. Mater.* **8** (1996) 1784.
4. R. H. KODAMA, A. E. BERKOWITZ, E. J. McNIFF. JR and S. FONER, *Phy. Rev. Lett.* **77** (1996) 394.
5. S. K. KHANNA and S. LINDEROTH, *Phys. Rev. Lett.* **67** (1991) 742.
6. R. N. BHOWMIK, R. RANGANATHAN, S. SARKAR and C. BANSAL, *Material Science and Engineering* A **326** (2001) 128.
7. D. J. FATEMI, V. G. HARRIS, M. X. CHEN, S. K. MALIK, W. B. YELON, G. J. LONG and A. MOHAN, *J. Appl. Phys.* **85** (1999) 5172.
8. H. H. HAMDEH, J. C. HO, S. A. OLIVER, R. J. WILLEY, G. OLIVERI and G. BUSCA, *ibid.* **81** (1997) 1851.
9. V. SEPELAK, S. WIβMANN and K. D. BECKER, *J. Magn. Magn. Mater.* **203** (1999) 135.
10. L. BIANCO, A. HERNANDO, E. BONETTI and E. NAVARRO, *Phys. Rev.* B **56** (1997) 8894.
11. QI CHEN and Z. J. ZHANG, *Appl. Phys. Lett.* **73** (1998) 3156.
12. V. A. M. BRABERS, Hand book of Magnetic Materials, Vol. 8, edited by K. H. Buschow (1995) p. 189; S. KRUPIKA and P. NOVAK, "Ferromagnetic Materials," Vol. 3, edited by E. P. Wolfarth (North-Holland, 1982) p. 189.
13. S. A. OLIVER, H. H. HAMDEH and J. C. HO, *Phys. Rev.* B **60** (1999) 3400.
14. Z. X. TANG, C. M. SORENSEN, K. J. KLABUNDE and G. C. HADJIPANAYIS, *Phys. Rev. Lett.* **67** (1991) 3602.
15. P. J. VAN DER ZAAG, A. NOORDERMEER, M. T. JOHNSON and P. F. BONGERS, *ibid.* **68** (1992) 3112.
16. V. A. M. BRABERS, *ibid.* **68** (1992) 3113.
17. B. D. CILLITY, "Elements of X-Ray Diffraction," 2nd ed. (Addison-Wesley, 1977).
18. A. RAY, A. CHAKRAVARTI and R. RANGANATHAN, *Rev. Sci. Instrum* **67** (1996) 789; A. CHAKRAVARTI, R. RANGANATHAN and A. K. RAYCHAUDHURI, *Pramana—J. Phys.* **36** (1991) 231.
19. G. F. GOYA and H. R. RECHENBERG, *J. Phys: Condens. Matter.* **10** (1998) 11829; G. F. GOYA, H. R. RECHENBERG and J. Z. JIANG, *J. Magn. Magn. Mater.* **218** (2000) 221.
20. R. JENKINS, R. GOULD and D. GEDCKE, "Quantitative X-ray Spectrometry" (Dekker, New York, 1981) p. 445.
21. J. L. DORMAN and D. FIORANI (eds.) "Magnetic Properties of Fine Particles" (North-Holland, 1991).
22. D. FIORANI, J. L. DORMAN, R. CHERKAOUI, E. TRONC, F. LUCARI, F. D'ORAZIO, L. SPINU, M. NOGUES, A. GRACIA and A. M. TESTA, *J. Magn. Magn. Mater.* **196/197** (1999) 143.
23. R. N. BHOWMIK and R. RANGANATHAN, *ibid.* **248** (2002) 101.
24. G. A. PETITT and D. W. FORESTER, *Phys. Rev.* B **4** (1971) 3912.

Received 6 November 2001
and accepted 23 April 2002